Study of the volatilization of Cesium and Rhenium in the waste vitrification process

Thomas Charpin, Alain Ledoux, Caroline Michel, Sophie Schuller, Dominique Thomas

Title

Study of the Volatilization of Cesium and Rhenium in the Waste Vitrification Process

Author names and affiliations

Thomas Charpin[1,2], Alain Ledoux[1], Caroline Michel[1], Sophie Schuller[1], Dominique Thomas[2]

[1] CEA, DES, ISEC, DE2D, SEVT, LDPV, Univ Montpellier, Marcoule, France

[2] Université de Lorraine, CNRS, LRGP, F-54000 Nancy, France

Corresponding author: thomas.charpin@protonmail.com

Abstract

A side effect of high level waste vitrification at 1100°C is the volatilization of radioactive cesium (Cs), recaptured further on in the process as a solid aerosol by a dust scrubber. Feedback from industry suggests that Cs combines with technetium (Tc) – simulated here by rhenium (Re), chosen for its similar behavior – to form volatile species. This work characterized Cs volatilization and aerosol formation. The first experiment involved elaborating and analyzing a simplified glass enriched with Cs and Re, which reinforce the volatilization phenomena. The results showed that a demixed liquid phase rich in Cs, Re, Mo, and Na formed in the liquid melt, which is reminiscent of a molybdic phase evoked in the literature. Moreover, analyzing the condensed gases led to the conclusion that the alkalis and Re volatilize congruently at around 700°C. In the second experiment, a series of measurements of the gas phase characterized aerosols throughout the process. The size distribution results showed that the particles formed in the furnace were mostly submicronic, and that the aerosols in the calciner and the dust scrubber included nanoparticles and micronic particles. SEM-EDS characterization revealed the composition of a spherical particle from the furnace made of two nested phases: one rich in Cs-Re-O, and the other rich in Na-Mo-O. The analyses performed showed that Cs and Re could be found in every particle sampled throughout the process, and that the micronic particles might originate from the aggregation of submicronic particles because of composition similarities. Thus, the observations led to a better understanding of the behavior of the elements of interest in both the melt and the gas phase.

Keywords: cesium, rhenium, technetium, particle, aerosol, volatilization, waste, vitrification

Body of paper

1. INTRODUCTION

As part of its long-term strategy, France uses vitrification as the key process to immobilize nuclear waste from fission power plants [1]. Uranium fission waste includes a wide spectrum of radiotoxic isotopes, which must be integrated within a glassy matrix. France developed a pioneering continuous 2-step process working at a temperature of 1100°C to synthesize nuclear glass [2-4], in operation at the waste reprocessing plant of La Hague. This is an all-inclusive process, performing all the nuclear waste treatment steps from calcination at 400°C through to vitrification at 1100°C. An additional dust scrubber captures airborne particles to reinject them into the calciner, as shown in Figure 1.

Figure 1. Flowsheet of the French vitrification process

A small amount of radioactive cesium (Cs) from the waste tends to volatilize from the furnace to the dust scrubber in the form of a solid aerosol [5-7]. Results from literature show that the fission product technetium (Tc) in the glass melt congruently volatilizes with the fission product Cs through complex interaction phenomena, and makes a major contribution to Cs escape [5][8-10]. In oxidizing conditions, Tc is a fission product normally found in the melt in the form of Tc^{+7} and Tc^{+4} [8][11-12]. A previous work from Cains [5] showed that the volatilization of Cs is congruent with that of Tc from 600°C to 1050°C. Moreover, the volatilization phenomenon is equimolar at 600°C, suggesting the formation of cesium pertechnetate, $CsTcO_4$. Recent works by Kim and Donald [8-9] have shown the co-vaporization of Cs and Tc, which can associate to form $CsTcO_4$ in solid particles. Thus, Cs volatilization is congruent with Tc volatilization, i.e. Cs and Tc combine and volatilize at the same time.

Previous work and literature reviews have also shown that Re can simulate Tc for work under non-radioactive oxidizing conditions, because of its similar behavior. In such cases, Tc and Re are mainly in the forms Tc^{+7} and Re^{+7} [8][11-12]. Re is better than Mn, W, Cr, Mo, or Ru in simulating Tc, in terms of similarities in chemistry, ionic size, speciation in glass, and volatility [8]. Re was used as a substitute for Tc in the R&D experiments described here, as it is currently considered the best simulant.

Due to the presence of various alkalis in the glass melt (Li, Na, K, Cs, Rb), Gassman and Weaver [13-14] conducted a series of experiments leading to the conclusion that there may be a competition between the alkalis (in the form of single-charge cations: X^+) to form volatile alkaline perrhenates ($XReO_4$). That implies that there is a volatilization congruence between alkalis and Re. The authors evoked an ion exchange phenomenon occurring in the melt. The affinity of the diverse alkalis to link with Re depends on their atomic radius, i.e. their inherent electronegativity.

The literature is rich in chemical data related to waste vitrification, whereas it is quite poor in data concerning aerosol formation during the process. The work described here presents a set of experiments designed to characterize the mechanisms of Cs/Re volatility (in non-radioactive conditions). The experiments aimed at characterizing the chemical combinations in the melt, which provoke the volatilization of Cs through the formation of aerosols. The work is innovative in that it shows the chemical composition and the size distribution of the solid particles formed during the process. In this paper, two different complementary experiments will be presented. The first experiment concerned the effect of Cs-Re matrix spiking. The goal was to highlight the formation of a demixed phase rich in Cs in a simplified glass, and the volatilization of the elements of interest. The second experiment focused on the aerosols formed during the vitrification process. The goal this time was to show the physical and chemical profiles of a typical Cs-type aerosol sampled in a vitrification process.

The combination of the results from the two experiments enabled the volatilization of Cs to be characterized. All of the experiments described in this paper were carried out with simulated glass in simulation mock-ups. Although the results cannot be directly applied to the industrial process, they contribute to an understanding of the volatilization phenomena that occur in this process.

2. EXPERIMENTAL

The experiments were performed on vitrification simulation process lines. The protocol included formulating a simulated waste solution at the laboratory, then performing calcination in order to obtain a calcine powder, and finally vitrifying the calcine. The two experiments related here involved two

different methods, but the results are complementary in better understanding Cs volatilization phenomena.

2.1. The two-step discontinuous glass preparation in small-scale processes

Multiple processes were used to perform the first experiment: a Small-Scale Calciner (SSC – see Appendix A) to calcinate the waste solution at 400°C, and a 1-kg furnace mock-up called Solidification TREAtment Mock-up (STREAM – see Appendix B) to prepare glass at 1100°C. Thus, it is a two-step discontinuous vitrification of the waste. Two glasses were prepared respecting the same protocol, with a difference in their Cs and Re concentrations. The goal was to observe potential phase demixions in glass, and to follow the volatilization of the elements of interest. The difference in concentration between the two matrices helped in characterizing the effect of Cs and Re on volatilization phenomena.

Before formulating a simulant waste solution, it was necessary to design the final glass matrix. The two matrices were simplified, with a limited number of elements in order to meet the laboratory safety requirements, but were representative of the reference matrix behavior in terms of volatilization phenomena. This required the conservation of the main elements of interest, which are listed below:

- Network formers: silicon (Si) and boron (B).
- Elements under study: cesium (Cs) and rhenium (Re).
- Other alkalis: sodium (Na) and lithium (Li), because of the supposed competition to form volatile alkali perrhenates [13-14]. In addition, there is always some potassium (K) present, due to glass frit impurities (about 0.2 wt%).
- Aluminum (Al), calcium (Ca), and zirconium (Zr), because they help to keep the appropriate rheological properties of the glass melt, and particularly a viscosity representative of the industrial glass.
- Molybdenum (Mo), because it is known to be volatile, and because of the potential formation of a molybdic phase in the glass melt. [15-21]
- Barium (Ba), because it helps to stabilize Mo in the glass melt, and to avoid demixion due to apatite crystallization [22].

- Iron (Fe), because it contributes to the calcine denitration phenomenon, and it balances the global redox of the glass melt.
- Zinc (Zn), that can lower the volatility of Cs by the formation of non-volatile species [23].
- Neodymium (Nd), because it is used as a simulant of minor elements in nuclear glass.
- Palladium (Pd) and ruthenium (Ru), representing the platinum group metals that can separate from the glass melt and form inclusions [22]. Moreover, Tellurium (Te) was added because it can form insoluble alloys with those elements.

The two matrices prepared were named Slightly Spiked Glass (SSG) and Highly Spiked Glass (HSG) because of the difference in Cs and Re spiking. A pre-selected glass frit was used to synthesize the glass. A specific "frit/glass" (F/G) ratio was applied. In each case, a simulated waste solution was previously formulated to prepare the calcine. It was an aqueous solution of nitric acid containing all of the selected elements, introduced in their nitrated form. Table 1 shows the nature of the components of the waste solution, the composition of the resulting calcine, the composition of the glass frit, and the composition of the final elaborated glass.

Table 1. Formulation of the Slightly Spiked Glass (SSG) and the Highly Spiked Glass (HSG)

Five liters of solution were prepared in a flask with a total concentration of 160 g/L of oxide-element equivalent. The next step was the calcination of this solution using the SSC. Some photos of this equipment are shown in Fig. A.1 and Fig. A.2, as well as a basic diagram of its structure in Fig. A.3. The calciner includes four heating zones. The solution feed rate into the calciner was 1 L/h, and an additional 166 g/L sugar solution was fed respecting a 0.1 L/h flow to help in the calcine fragmentation. The calciner rotated at 55 rpm during the steady state. The heat increased gradually as the solution flowed along the tube, drying and calcinating the solution. The temperature reached 400°C at the outlet. A dry powder called "calcine" was thus obtained. There was a 350 L/h sweeping air flow in the calciner. The calcine was continuously collected in a tank for 5 hours. Afterwards, the calcine was ground and mixed with an appropriate quantity of fresh glass frit using a precision balance, and respecting the "F/V" value (Table 1). A three-dimensional mixer was used for 2 minutes to homogenize the powder mixture. The product was then ready for vitrification.

The vitrification was performed in the STREAM furnace (Fig. B.1), which works with three heating resistors. In this study, the STREAM did not include any impeller or bubbling system to homogenize the glass melt, so the previous three-dimensional mixing step was very important. Part of the calcine and glass frit mixture was previously placed in an Inconel® can in order to elaborate 1 kg of glass. The can was placed in the oven, and was hermetically sealed with a jacketed water-cooled lid. The vitrification heating program included a 300°C/h ramp from ambient temperature to 1100°C, and a 2-hour temperature plateau at 1100°C. The gases formed during the experiment were channeled to a downstream gas treatment unit composed of a dust-scrubber and a condenser, which stayed in operation from the beginning to the end of the experiment. The dust scrubber was a column with perforated trays, and was continuously sprayed with 95°C water that captures the particles. The condenser was a sprayed double-pass cooled system that condensed the gas formed. The solution from the dust scrubber, and the condensed vapors from the condenser, were sampled every 30 min during the vitrification. Then all samples were analyzed by ICP-AES, enabling the volatility of every element from the glass melt to be quantified. The volatilization profiles were plotted over time.

At the end of the heating program, the resistors were turned off but the cooling water continued to flow in the furnace lid. Thus, the glass cooled slowly at about 1°C/min. The material was then cut, and characterized using SEM-EDS and XRD techniques. Therefore, this experiment enabled the observation of volatile phenomena and chemical-in-melt behavior.

2.2. The continuous glass preparation in the pilot-scale process

The second experiment was designed to characterize the Cs-bearing aerosols as they passed through the vitrification process. A Pilot-Scale Mock-Up (PSMU) including a calciner, a furnace, and a dust scrubber was used to prepare a Typical Simulant Glass (TSG). The PSMU is a continuous process that can perform all the steps of nuclear waste vitrification, as shown in Fig. 1. The compositions for the synthesis of the TSG are shown in Table 2.

Table 2. Formulation of the Typical Simulant Glass (TSG)

The experiment involved a continuous feed into the rotating calciner of 10.5 L/h of simulated waste solution, and 1 L/h of sugar solution. The liquid flowed through the hot calciner (Fig. A.3), for the evaporation of water and the denitration of the waste, then the calcination at 400°C. At the end, the calcine powder fell into a 30-kg capacity furnace. A flow of 1 kg/h to 5 kg/h of fresh glass frit was also fed into the furnace. The calcine and the frit were mixed together at the calciner outlet, and the mixture was homogenized in the furnace with an 80-rpm rotating impeller. This is a three-zone furnace, with three resistors that heat the crucible walls to the desired temperature. The mixture of powders was heated to 1100°C, ensuring powder melting and the incorporation of the waste into the glass. A 200-NL/h bubbling system injected air into the glass melt and helped in the overall homogenization. Some of the elements present in the melt volatilized in the form of a solid aerosol, channeled up from the furnace to the calciner, then to the dust scrubber. It cannot be excluded that there was some volatilization in the calciner, but our previous work showed that this would be minor. The dust scrubber was a contacting column that captured the aerosol. It contained acidic water at 105°C, which sprayed the trays. The aerosol particles that flowed through the dust scrubber struck the trays and the walls of the column, where they were captured. Any residual aerosol was channeled out to a downstream gas treatment unit to be fully recovered. The particles captured in the dust scrubber solubilized in the acidic solution, which was partly recycled to the calciner (1 L/h) in order to vitrify the totality of the waste matter.

The goal of the experiment was to sample and analyze the aerosols that flow through the process during vitrification. Figure 2 shows the set up designed for aerosol sampling and analysis, used to characterize particles.

Figure 2. Experimental set up for aerosol sampling on the PSMU

The aerosols produced during the vitrification process were sampled through a nozzle placed at the sampling point in such a way that the kinetic energy of the particles was conserved. From there, they were channeled to a diluter DI-1000 through a hose heated to 200°C. The heat helped prevent gas condensation and particle deposition. Hot compressed air was pumped into the dilutor to lower the particle concentration and avoid any downstream device saturation. Next, the diluted aerosols were channeled to an ELPI+ cascade impactor, to separate the particles by size [24]. Aerosol particles were

collected on a succession of trays, and were quantified by conductivity detection. The main advantage of the ELPI+ device is that particles can be recovered from the trays for additional SEM-EDS analyses.

This experimental set up is mobile, which allowed measurements to be performed at each step of the vitrification process. Figure 3 shows the locations of the sampling points.

Figure 3. Sampling points on the PSMU

Sampling started after the steady state was reached on the PSMU. The first sampling point (a) was at the furnace gas outlet, the second (b) was at the calciner gas outlet, and the third (c) was at the dust-scrubber gas outlet. Characterizing aerosols at points (a), (b), and (c) helped to understand the mechanisms of particle formation, and their behavior during the process. Although, the temperature was about 1100°C in the furnace, 400°C in the calciner, and 105°C in the dust scrubber, the temperature of the aerosol carrier gas was lower. Table 3 gives important data concerning the gas temperature and gas flow measured at each sampling point.

Table 3. PSMU process data

3. RESULTS

3.1. Characterization of glass syntheses in the STREAM

Two simplified glass matrices were prepared in the STREAM mock-up respecting the protocol described in §2.1. After cooling, the resulting pieces of glass were cut by hand saw using water as a cooling fluid. Figure 4 shows the glass with low concentrations of Cs (0.9 wt%) and of Re (0.3 wt%). This glass is globally homogenous, with some occasional scattered micronic metallic inclusions corresponding to insoluble Ru and Pd.

Figure 4. Glass slightly spiked in Cs and Re

Next, we observed the effect of an extreme spiking in Cs and Re. Figure 5 shows the glass with high concentrations of Cs (2.2 wt%) and of Re (1.8 wt%). A white solid, demixed from the glass, tended

to dissolve in water during the cutting. Some round holes could be observed at the bottom of the crucible, with the white solid inside.

Figure 5. Glass highly spiked with Cs and Re

SEM-EDS mapping performed in this white solid (Fig. 6) reveals that it consisted of Cs, Re, Na, O, and Mo, with some inclusions of Ca. It should be noted that Li cannot be detected by SEM-EDS. Cs and Re seem to be coupled, as well as Mo and Ca. The identification of structures like $CsReO_4$, $NaReO_4$, and Na_2MoO_4 could be determined in this phase by XRD (Fig. 7).

Figure 6. SEM-EDS mapping of the white solid phase

Figure 7. XRD-diffractogram from the analysis of the white solid powder

3.2. Characterization of the volatilized species during glass synthesis in the STREAM

The different species volatilized during the glass elaboration in the STREAM furnace - coupled with a gas recovery unit - were detected. The ICP-AES analyses were able to determine the evolution of the volatilization of the elements of interest during the elaboration of the HSG (Fig. 8). The evolution of the estimated temperature of the glass melt with time was also followed, by approximation from the heating resistor temperature.

Figure 8. Volatilization flows of the elements of interest compared to Re during the elaboration of a simplified spiked glass

There was a clear congruence between the volatilization of the alkalis and that of Re, with simultaneity from 3 hours after the beginning of the experiment. The volatilization of the alkalis started at about 700°C and reached a maximum at about 1000°C. The volatilizations of Li, Na, K (frit impurity), and Cs seem to be synchronized with the Re volatilization. Furthermore, Fig. 8 shows the volatilization flows of Mo and Pd. These flows are multiplied by 100 to be observable on the graph, because the quantity volatilized is negligible compared to that of the alkalis. There is no synchronization between the flow of Mo compared to the flow of Re, so the volatilization was not congruent. The early peak between 20°C and 90°C was certainly induced by a pollution in the condensate sample, and need not be considered.

Furthermore, Mo appeared to volatilize from 250°C, which is a considerably lower temperature than that of Re and the alkalis. It was noted that there was strictly no volatilization of the Pd, which is a good control element for volatility.

3.3. Characterization of the aerosol size distribution in the vitrification PSMU

The aerosols formed in the PSMU during the TSG synthesis (see protocol in §2.2) were sampled and analyzed using a specific experimental set up. Thus, data was obtained related to the aerodynamic diameter[1] of the particles, as shown in Fig. 9. All of the bar charts presented here were plotted as a function of particle number distribution. The graphs reveal the presence of more than one population.

Figure 9. Particle size distribution of the aerosols sampled at different locations

Figure 9.A shows a bimodal distribution of the aerosols formed in the furnace, with a major population around 0.04 µm (2.3E8 cm^{-3}) and a minor one around 0.5 µm (3E7 cm^{-3}). Both of the populations were submicronic, and most of the particles were smaller than 0.1 µm. The total number of particles was 6.26E8 cm^{-3}.

Figure 9.B shows a bimodal distribution of the aerosols sampled in the calciner, with a first peak around 0.01 µm and a minor peak around 2 µm. It can be seen that there were submicronic and micronic populations. The total particle concentration in the calciner (2.80E6 cm^{-3}) was lower than in the furnace. Here, the submicronic-field peak was capped at 7.5E5 cm^{-3} and the micronic-field peak at 5.5E5 cm^{-3}.

Figure 9.C shows a bimodal distribution of the aerosols sampled at the dust scrubber outlet. The peak locations are quite similar to the calciner graph, because they were located at around 0.01 µm and 2 µm. The peaks were respectively capped at 4.8E5 cm^{-3} and 2.2E5 cm^{-3}, and the total number of particles was about 1.13E6 cm^{-3}, which is lower than the calciner values.

[1] The aerodynamic diameter of a particle is defined as the diameter of a spherical particle having a density equal to 1 and the same settling velocity as the particle under consideration.

3.4. Characterization of the morphology and chemical composition of the aerosols

Sampling and segregation of the particles by the ELPI+ impactor enabled them to be recovered, and then analyzed by SEM and EDS. Here, the goal was to identify the composition of the particles. This was an element speciation only, and no structures were identified. SEM image acquisition enabled the morphology of the particles to be observed at each sampling point. The images obtained by SEM highlight the chemical contrast between the different phases in the solid aerosol.

Figure 10 shows irregular-shaped submicronic particles from the furnace. Two phases can be observed: a bright phase (heavy) and a darker phase (light). These two phases seem to be mostly separated, but they can be somewhat aggregated. Because the chemical contrast is different, Fig. 10 suggests that the composition of the phases may not be the same. The elemental detection performed on the phases by an EDS system allowed the nature of the elements in the particles to be determined. Figure 11 reveals that the bright phase contains mainly Cs, Re, and O, with a little peak of Na. In addition, some traces of Ru, Te and Mo were detected. The nature of the dark phase is of interest. Analyzing this phase was difficult, because it tended to disintegrate when bombarded with electrons (analysis n1 in Fig. 10). Thus, obtaining a spectrum has so far been impossible because of the physical instability.

Figure 10. Morphology of submicronic particles from the furnace, observed with SEM

Figure 11. SEM-EDS spectra from Analysis n2 on Fig. 10

Figure 12 shows spherical micronic particles from the furnace. Most of them have a smooth surface, but a few are spiky. The latter particles appear bitonal: bright and dark. It seems that there are multiple nested phases forming the spheres. EDS chemical characterization helped to clarify that point. Figure 13 shows a SEM-EDS mapping of a round micronic particle, and two nested phases can be observed in the BSE image. The elements identified are Cs, Re, and O in the heavy phase, with Na, Mo, Ru, and O in the light phase.

Figure 12. Morphology of micronic particles from the furnace, observed with SEM

Figure 13. SEM-EDS mapping of a micronic particle from the furnace

Figure 14 shows micronic particles from the calciner. These polyhedrons are clearly different from the round particles observed in the furnace. As before, it is possible to see two different shades of chemical contrast: bright and dark. The SEM-EDS analyses revealed the presence of Cs-Re in the bright phase (Fig. 15), whereas the dark phase disintegrated under the effect of the electron beam.

Figure 14. Morphology of micronic particles from the calciner, observed with SEM

Figure 15. SEM-EDS spectra from Analysis n4 on Fig. 14

Figure 16 sought to show micronic particles from the dust scrubber, but no particles can be observed. This image shows a chemical layer with fissures and a scattering of micronic bright inclusions characterized by EDS as Cs-Re particles (Fig. 17). Here again, these two elements were found to be prevalent.

Figure 16. Morphology of micronic particles from the dust scrubber, observed with SEM

Figure 17. SEM-EDS spectra from Analysis n1 on Fig. 16

4. DISCUSSION

4.1. General mechanism of Cs and Re volatilization

The HSG prepared in the STREAM (Fig. 5) revealed typical singularities induced by the high concentrations of Cs and Re. The spherical holes observed at the bottom of the crucible were certainly due to bubbles formed in the glass melt during its elaboration, though there was no bubbling system in the furnace. The white phase could only be observed for the HSG, and was not found in the SSG (Fig. 4). Its formation was certainly due to the limitation of solubility. Riley showed that the solubility of Re in Handford glass is only about [ReO_2] = 0.35 wt% [25], whereas in this study the concentration was 1.8 wt% in the HSG and 0.30 wt% in the SSG (Table 1). The presence of cesium perrhenate ($CsReO_4$ – Fig. 6) in the white solid is reminiscent of the formation of cesium pertechnetate ($CsTcO_4$), as described in the literature [5]. This confirms that Re (or Tc) certainly has an impact on the volatility of Cs. Moreover, the presence of sodium perrhenate ($NaReO_4$) indicates that Re can combine with various alkaline elements in the melt. This suggests a possible competition between the alkalis, as mentioned earlier [13-14]. Lastly, the Mo found in the white phase suggests a possible mixing with Ca, Cs, Na, and

Re in a liquid molybdic phase during glass synthesis (attracting cations from the calcine), and then a crystallization after cooling ($CsReO_4$, $NaReO_4$, Na_2MoO_4, $CaMoO_4$). Volatilization could come from the formation of gaseous species (Mo, Cs, Re, O, Ru) because of the low melting temperature of this phase and the main compounds present (Na_2MoO_4 - 680°C -, $CsReO_4$ - 620°C -, $NaReO_4$ - 420°C -, $LiReO_4$ - 419°C -, $KReO_4$ - 551°C -) [26-27]. Moreover, it has to be remembered that the vaporization temperature of eutectics is certainly low compared to that of pure components.

The volatilization study during the HSG synthesis was of interest because the analyses performed on the gas treatment unit solutions revealed co-volatilization phenomena (Fig. 8). The synchronization between alkali volatility and Re volatility was consistent with the literature claims concerning $CsReO_4$ formation and alkali competition [5][13-14]. All vapor flows decrease once the maximum temperature has been reached, forming volatilization peaks. These peaks are related to the main steps of the dissolution reaction of calcine in glass frit, whereas the volatility decrease concerns the glass refining phase [15][28]. There is a denitration of the waste elements when the calcine incorporates into the glass network. In particular, residual sodium nitrates ($NaNO_3$) not decomposed during calcination (400°C), and with a low melting temperature (306°C), might decompose at 600°C and volatilize at around 700°C [29-30].

Thus, the experiment on the STREAM helped to identify some of the volatile components as alkali perrhenates, and a volatilization congruency was observed from 700°C. The experimental results also suggest that the volatilization of Cs, Re, and Na might be increased by the formation of a molybdic phase in the glass melt, transported to the surface by bubbles.

4.2. Critical analysis of the physico-chemical characteristics of the aerosols

The characterization of the aerosols performed on the PSMU during the TSG synthesis gave a clear representation of the evolution of particle size throughout the vitrification process (Fig. 9). Before comparing the results, it is necessary to consider the presence of micronic water droplets (diameter > 0.320 µm) in the aerosols sampled at the outlet of the calciner and the dust scrubber, despite the sampling hoses being heated to 200°C. This was due to the high humidity in the process atmosphere

at those points. It was supposed that the flying droplets might lead to an overestimation of the number of micronic particles, which might slightly skew the distribution. This phenomenon explains why the standard deviations are big for those sampling points. On the contrary, the atmosphere of the furnace was dry, and therefore there would not have been water vapor present.

The aerosols at the calciner outlet result from a mixture of the aerosols channelled from the furnace and those formed in the calciner (Fig. 1). The population of micronic particles in the calciner (2 µm) had a bigger diameter than that in the furnace (0.5 µm). Apart from the influence of flying water droplets, this could be because some particles from the furnace agglomerated. The decrease in the total number of particles could also result from the phenomenon of wall deposition. An illustration of this is the thick layer of chemicals that is often recovered from the walls in the industrial process. Moreover, the comparison of Fig 9.B and Fig. 9.C shows that more than half of the total number of particles were captured. That highlights the efficiency of the dust scrubber in capturing such particles. Particle deposition and particle agglomeration might still remain between the calciner and the dust scrubber, but these two phenomena would have a minor influence, given the configuration of the process.

The SEM images differ considerably from one sampling point to another. They help to understand the behavior of the particles during the process. As the atmospheric conditions in the furnace, in the calciner, and in the dust scrubber were not the same, the further the aerosol went in the process, the more and more humid the carrier gas became. The presence of acidic water could dissolve the sampled particles once they struck the plates of the ELPI+ device. This can explain the difference in morphology observed. Because of the dry atmosphere in the furnace, the particles sampled were directly representative of the aerosols in it (Fig. 10 and Fig. 12). The atmosphere in the calciner was more humid, and some of the matter collected on the recovery trays certainly dissolved and crystallized when drying, forming polyhedrons (Fig. 14). Finally, there was so much humidity and acid in the dust scrubber that the particles there completely dissolved to form a layer on the trays (Fig. 16).

The combination of the SEM images with EDS characterization gave a chemical overview of the aerosol quality. The presence of Mo in submicronic particles from the furnace (Fig. 11) might suggest a connection between Cs-Re volatilization and the formation of a molybdic phase in the glass

melt. The disintegration of the dark phase by the electron beam is typical of phases enriched in sodium, or more generally alkalis, which suggests the presence of Na in such phases. Furthermore, the observation of a spherical particle from the furnace (Fig. 13) revealed two nested phases (bright and dark). The SEM analysis established that Cs and Re were certainly coupled to form the bright phase. Moreover, it showed that Na was located in the dark phase, and that it might not be associated with Cs / Re. These observations are reminiscent of the SEM-EDS analyses performed on submicronic particles (Fig. 11), as concerned the bright and the dark phases. Thus, the micronic particles in Fig. 12 might be from an agglomeration of the submicronic particles observed in Fig. 10, which suggests that the big and the small particles may have the same composition. Other elements such as Mo and Ru can also be observed in Fig. 13. It would appear that Mo is located in the same place as Na, which suggests a Mo-Na-O association. This recalls the composition of the white demixed phase given in Fig. 6. It is thought that there is an single demixed liquid phase in glass at 600°C containing all these elements (Na, Cs, Re, Mo, O) [15][17]. This temperature matches the fusion temperature of alkaline perrhenates and alkaline molybdates. The phase crystallizes when cooling, forming complex species such as $NaReO_4$, Na_2MoO_4, and $CsReO_4$. It can be hypothesized that these chemical elements volatilized from the melt, and crystallized to form solid aerosol particles. If so, crystallization can happen under gaseous phase.

5. CONCLUSION

Merging the results obtained from the two experiments enabled characterization of the mechanisms of Cs volatilization during the calcination and vitrification processes.

A glass made with high concentrations of Cs and Re (HSG) produced a demixed white phase mostly composed of Cs and Re. This solid was contained in circular holes, suggesting the temporary presence of gas at the high vitrification temperature. The additional presence of Mo in this white solid suggests that the Cs-Re volatility might be linked with the formation of a molybdic phase, which may form at a lower temperature (600°C) than the Cs-Re volatilization point (700°C, estimated). The phase may dissolve cations in the melt, such as alkalis or perrhenates, and provoke demixing. The existence of this white phase was revealed thanks to the high concentrations of Cs and Re in the HSG. It can be

supposed that such a phase also exists at lower concentrations, but it might be incorporated into the glass during the elaboration.

The mass balances performed on the STREAM while making the HSG highlighted that there is a congruence between alkali volatilization and Re volatilization. There is a rise from 700°C up to the temperature of 1000°C, reflecting evaporation. It has been hypothesized that there is a competition between the alkalis to form gaseous alkaline perrhenates [13-14]. Furthermore, it has been shown that the volatilization of Mo and Pd is extremely low, and that there is no congruence with Re volatilization.

Further analyses of the particles sampled in the PSMU (TSG synthesis) led to the observation of two nested phases: one rich in Cs-Re-O, and the other rich in Na-Mo-O. It was striking to note the presence of Mo in the particles, suggesting a connection between the demixed white phase (from the HSG) and the formation of particles (from the TSG). In addition, Cs and Re were similarly distributed between submicronic particles and micronic particles, which may mean that all sizes have to be retained by the dust scrubber to reach the maximum Cs capture efficiency.

Observation of the aerosol size distribution in the PSMU revealed that the particles evolved while flowing through the process. While distribution was bimodal and submicronic in the furnace (two peaks at 0.04 µm and 0.5 µm), particles were globally bigger in the calciner and the dust scrubber, with a – minor in mass – submicronic population (0.01 µm) and a micronic population (2 µm). These results can be used to optimize particle capture in the downstream gas treatment unit.

Acknowledgments

This work was supported by funding provided by the French Atomic Energy and Alternative Energy Commission (CEA) and Orano group, through the VITHA project. The French vitrification process was developed by the Science and Technology Institute for the Circular Economy of Low Carbon Energies (ISEC), which is part of the CEA. The industrial process operates at the waste reprocessing plant of Orano, La Hague (France).

We would like to thank I. Giboire and E. Regnier from the Laboratory of Development of Conditioning Matrices (CEA/LDMC) for their help in understanding the particular phenomena associated with the formation of glass. We are grateful to R. Podor and J. Lautru for their help and their expertise in performing Environmental SEM on aerosol particles. We also express our gratitude to C. Roussel, A. Rodrigues, and H. Pablo from Orano for their industrial support during our project.

References

[1] Vernaz, E., and Bruezière, J., 2014, "History of Nuclear Waste Glass in France," Procedia Materials Science, 7, pp. 3-9. Doi: doi.org/10.1016/j.mspro.2014.10.002

[2] Vernaz, E., Gin, S., and Veyer, C., 2012, "Waste Glass," *Konings R.J.M.*, Comprehensive Nuclear Materials, eds., Elsevier, Amsterdam, vol. 5, pp. 451-483. Doi: doi.org/10.1016/B978-0-08-056033-5.00107-5

[3] Barba Rossa, G., 2018, "Modélisation Multiphysique de l'Élaboration de Verre en Creuset Froid," PhD dissertation, Université de Grenoble-Alpes, France, https://tel.archives-ouvertes.fr/tel-01860351

[4] Gruber, P., Tronche, E., et al., 2011, "Limited Increase of Particle Entrainment in the Off-Gas System of a Cold Crucible Induction Melter. Compared with a Joule-Heated Metal Melter for HLLW Vitrification," Proceedings of the WM2011, Phoenix, AZ, February 28 – March 3, 2011, Paper No. 11465, https://api.semanticscholar.org/CorpusID:138282090

[5] Cains, P.W., Yewer, K.C., and Waring, S., 1992, "Volatilization of Ruthenium, Cesium and Technetium from Nitrate Systems in Nuclear-Fuel Processing and Waste Solidification," Radiochimica Acta, 56(2), pp. 99-104. Doi: doi.org/10.1524/ract.1992.56.2.99

[6] Cains, P.W., and Yewer, K.C., 1986, "Fission Product Volatilisation in the Calcination and Vitrification of High-Level Wastes," Graham and Trotman, United Kingdom, pp. 766-776.

[7] Delorme, L., 1998, "Mécanismes de Volatilité des Verres et des Fontes Borosilicates d'Intérêt Nucléaire," PhD dissertation, Université d'Orléans, France.

[8] Kim, D., and Kruger, A.A., 2018, "Volatile Species of Technetium and Rhenium during Waste Vitrification," Journal of Non-Crystalline Solids, 481, pp. 41-50. Doi: doi.org/10.1016/j.jnoncrysol.2017.10.013

[9] Donald, I.W., 2010, "Waste Immobilization in Glass and Ceramic Based Hosts: Radioactive, Toxic and Hazardous Wastes," eds., Wiley-Blackwell. Doi: doi.org/10.1002/9781444319354.

[10] Childs, B.C., Poineau, F., et al., 2015, "The Nature of the Volatile Technetium Species Formed during Vitrification of Borosilicate Glass," Journal of Radioanalytical and Nuclear Chemistry, 306(2), pp. 417-421. Doi: doi.org/10.1007%2Fs10967-015-4203-5

[11] Pegg, I.L., et al., 2015, "Behavior of Technetium in Nuclear Waste Vitrification Processes," Journal of Radioanalytical and Nuclear Chemistry, 305(1), pp. 287-292. Doi: doi.org/10.1007/s10967-014-3900-9

[12] Lukens, W.W., McKeown, D.A., et al., 2007, "Dissimilar Behavior of Technetium and Rhenium in Borosilicate Waste Glass as Determined by X-Ray Absorption Spectroscopy," Chemistry of Materials, 19(3), pp. 559-566. Doi: doi.org/10.1021/cm0622001

[13] Gassman, P.L., McCloy, J.S., et al., 2014, "Raman Analysis of Perrhenate and Pertechnetate in Alkali Salts and Borosilicate Glasses," Journal of Raman Spectroscopy, 45(1), pp. 139-147. Doi: doi.org/10.1002/jrs.4427

[14] Weaver, J., Soderquist, C.Z., et al., 2017, "Chemical Trends in Solid Alkali Pertechnetates," Inorganic Chemistry, 56(5), pp. 2533-2544. Doi: doi.org/10.1021/acs.inorgchem.6b02694

[15] Boué, E., 2019, "Kinetic and Thermodynamic Factors Controlling the Dissolution of Molybdate-Bearing Calcines during Nuclear Glass Synthesis," Journal of Nuclear Materials, 519, pp. 74-87. Doi: doi.org/10.1016/j.jnucmat.2019.03.037

[16] Short, R.J., 2014, "Phase Separation and Crystallisation in UK HLW Vitrified Products," Procedia Mater. Sci., 7, pp. 93-100. Doi: doi.org/10.1016/j.mspro.2014.10.013

[17] Pegg, I.L., Gan, H., et al., 2010, "Mitigation of Yellow Phase Formation at the Rokkasho HLW Vitrification Facility," Proceedings of the WM-2010, Phoenix, AZ, March 7-11, 2010.

[18] Rose, P.B., Woodward, D.I., et al., 2011, "Crystallization of a Simulated Borosilicate High-Level Waste Glass produced on a Full-Scale Vitrification Line," J. Non-Cryst. Solids, 357, pp. 2986-3001. Doi: doi.org/10.1016/j.jnoncrysol.2011.04.003

[19] Hand, R.J., Short, R.J., et al., 2005, "Molybdenum in glasses containing vitrified nuclear waste," Proceedings of the VII European Society of Glass Technology Conf., Athens, Greece, 25-28 April 2004, 46, pp. 121-124.

[20] Hyatt, N.C., Short, R.J., et al., 2005, "The Structural Chemistry of Molybdenum in Model High Level Nuclear Waste Glasses, Investigated by Mo K-Edge X-Ray Absorption Spectroscopy," Environ Issues Manage, Waste Tech. Ceram. and Nucl. Ind., 168, pp. 179-190. Doi: doi.org/10.1002/9781118408438.ch17

[21] Short, R.J., Hand, R.J., et al., “Environment and Oxidation State of Molybdenum in Simulated High Level Nuclear Waste Glass Compositions,” J. Nucl. Mater., 340(2-3), pp. 179-186. Doi: doi.org/10.1016/j.jnucmat.2004.11.008

[22] Chouard, N., 2011, "Structure, stabilité thermique et résistance sous irradiation externe de verres aluminoborosilicatés riches en terres rares et en molybdène," Ph.D. dissertation, Université Pierre et Marie Curie – Paris VI, France. Link: https://pastel.archives-ouvertes.fr/pastel-00644194

[23] Banerjee, D., Joseph, A., et al., 2012, “Effect of Composition and Temperature on Volatilization of Cs from Borosilicate Glasses,” J. Am. Ceram. Soc., 95(4), pp. 1284-1289. Doi: 10.1111/j.1551-2916.2012.05077.x

[24] Papastefanou, C., 2008, “Radioactive aerosols - Chapter 6 Aerosol Sampling and Measurement Techniques,” Elsevier, vol. 12, pp. 113-159. Doi: doi.org/10.1016/S1569-4860(07)12006-4

[25] Riley, B.J., McCloy, J.S., et al., 2013, “Crystallization of Rhenium Salts in a Simulated Low-Activity Waste Borosilicate Glass,” J. Am. Ceram. Soc., 96(4), pp. 1150-1157. Doi: doi.org/10.1111/jace.12280

[26] Sugawara, T., and Jin, K., 2018, “Enthalpy and Heat Capacity of Na2MoO4 and CaMoO4,” Thermochimica Acta, 669, pp. 185-193. Doi: doi.org/10.1016/j.tca.2018.09.011

[27] Lukas, W., and Gaune-Escard, M., 1982, “Temperatures and Enthalpies of Melting of Alkali-Metal Perrhenates,” The Journal of Chemical Thermodynamics, 14(6), pp. 593-597. Doi: doi.org/10.1016/0021-9614(82)90074-X.

[28] Dussossoy, J.L., Schuller, S., and Advocat, T., 2007, “The Formulation of New High Level Glasses with an Increased Waste Loading Charge,” Proceedings of the ICG 2007, Strasbourg, France.

[29] Sergeev, D., Reis, B.H., et al., 2019, “Thermodynamics of the Ca(NO3)2 – NaNO3 System,” Calphad, 67, 101688. Doi: doi.org/10.1016/j.calphad.2019.101688

[30] Paraiso, K., Sauvage, E., and al., 2020, “Characterization and Modeling of Chemical Reactions taking place during the Vitrification of High Level Nuclear Waste,” Thermochimica Acta. Paper submitted.

Figures and Tables

FIGURE SUMMARY

TABLE SUMMARY

APPENDICES

FIGURES

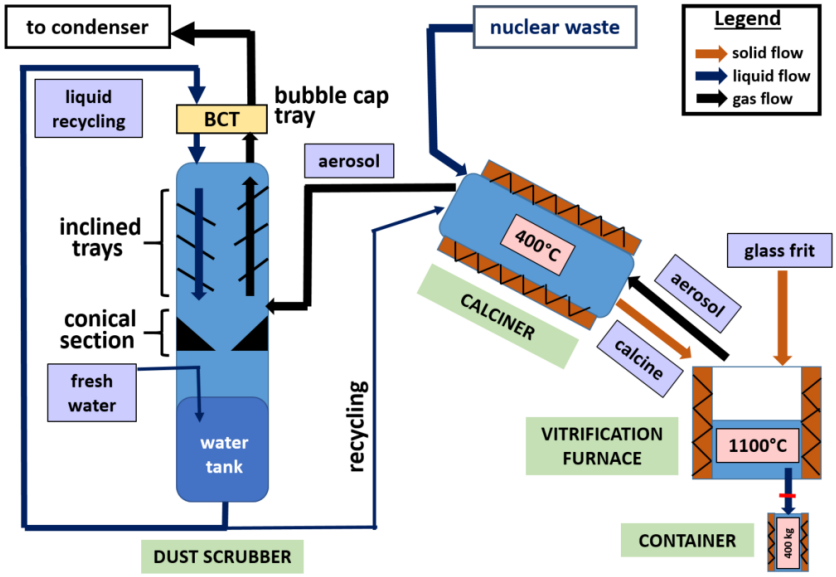

Figure 1. Flowsheet of the French vitrification process

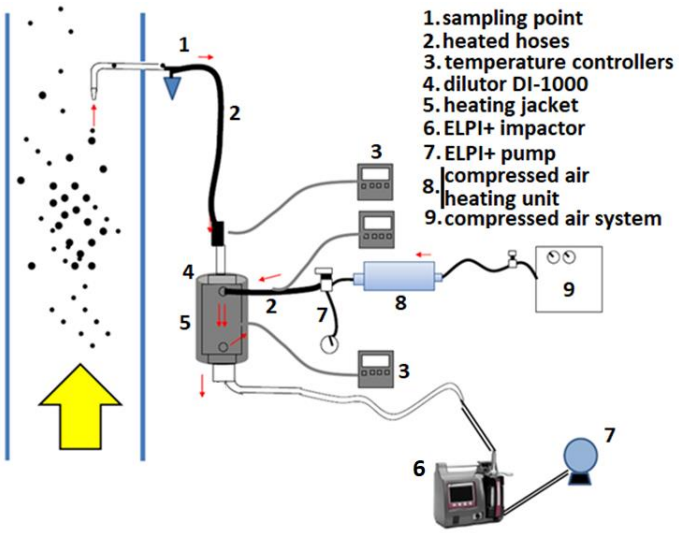

Figure 2. Experimental set up for aerosol sampling on the PSMU

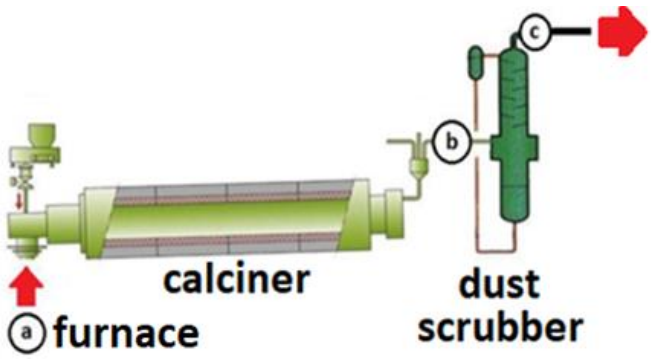

Figure 3. Sampling points on the PSMU

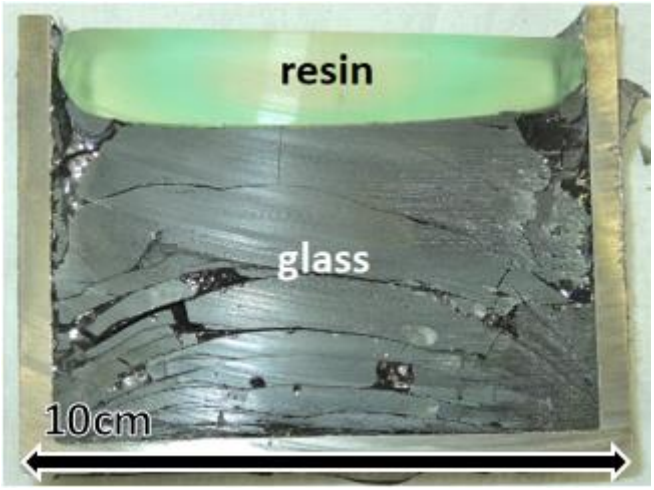

Figure 4. Glass slightly spiked in Cs and Re

Figure 5. Glass highly spiked with Cs and Re

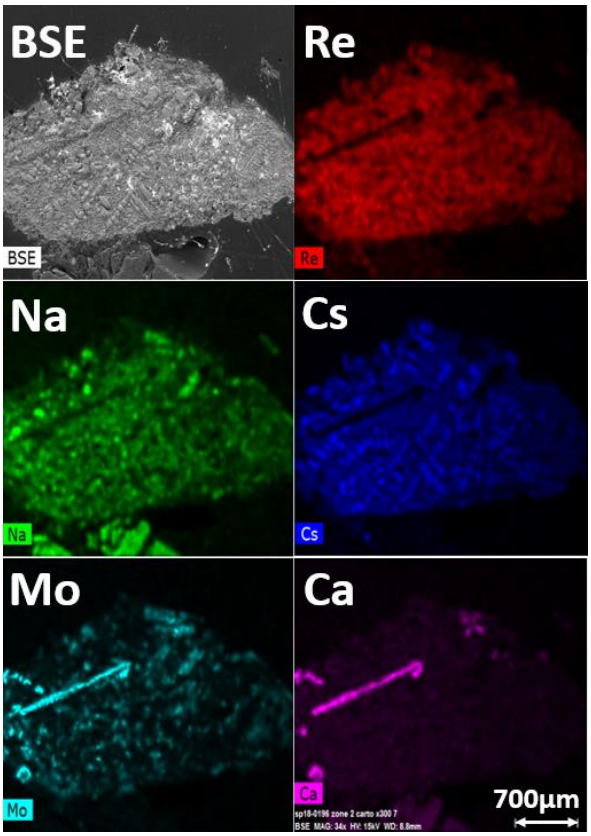

Figure 6. SEM-EDS mapping of the white solid phase

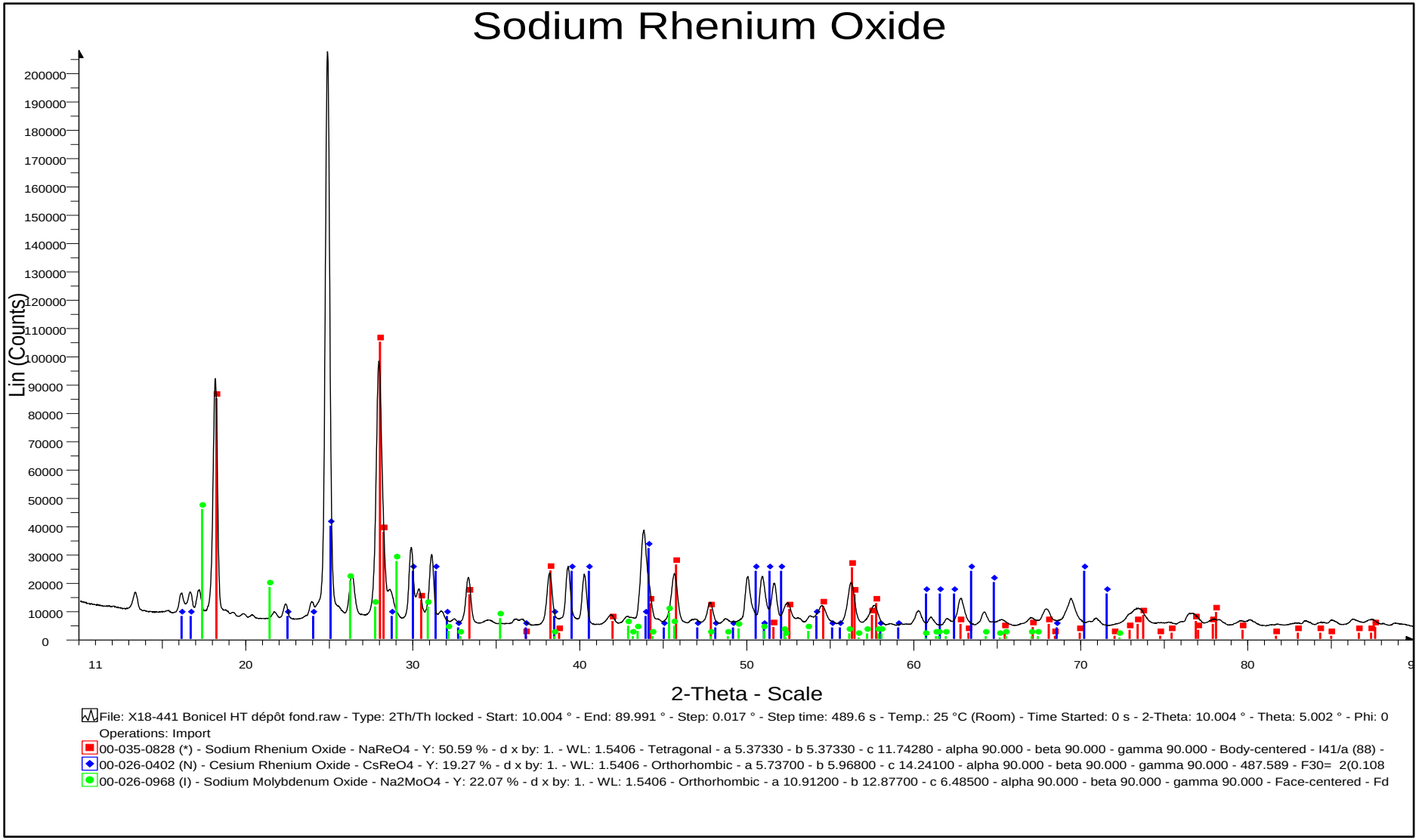

Figure 7. XRD-diffractogram from the analysis of the white solid powder

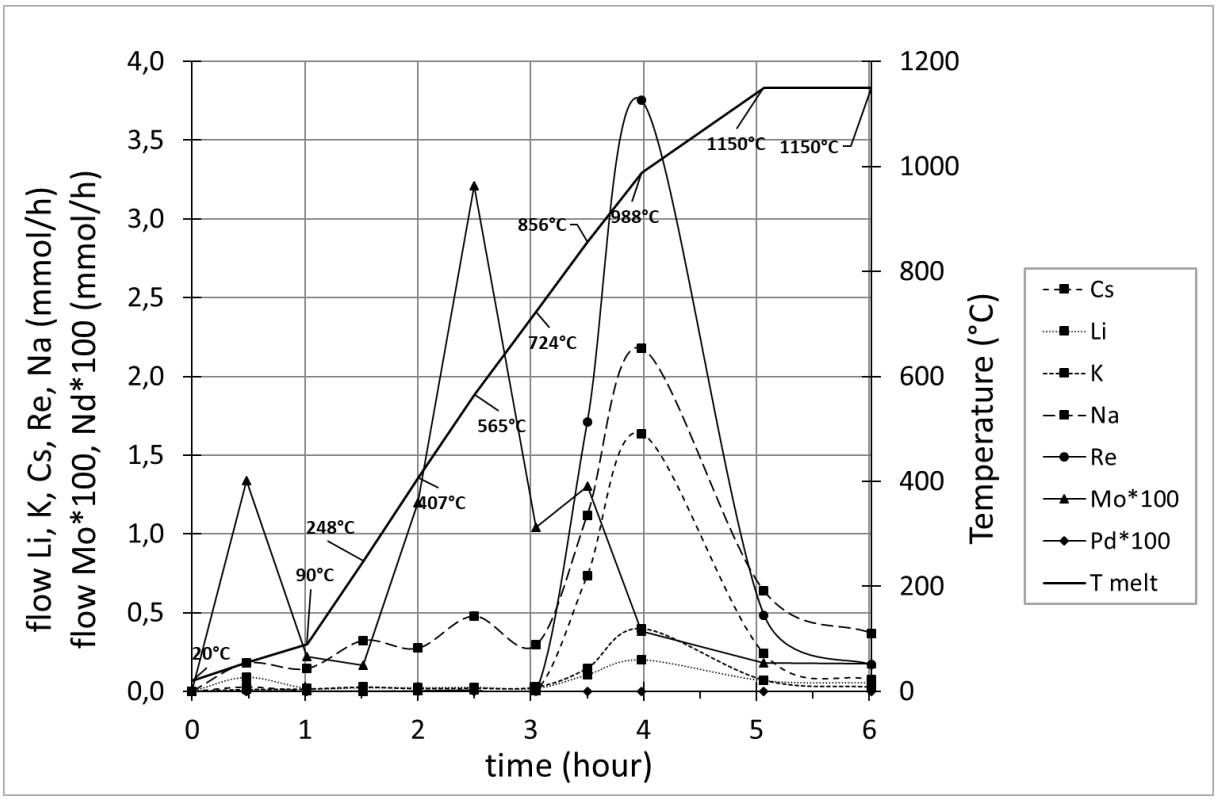

Figure 8. Volatilization flows of the elements of interest compared to Re during the elaboration of a simplified spiked glass

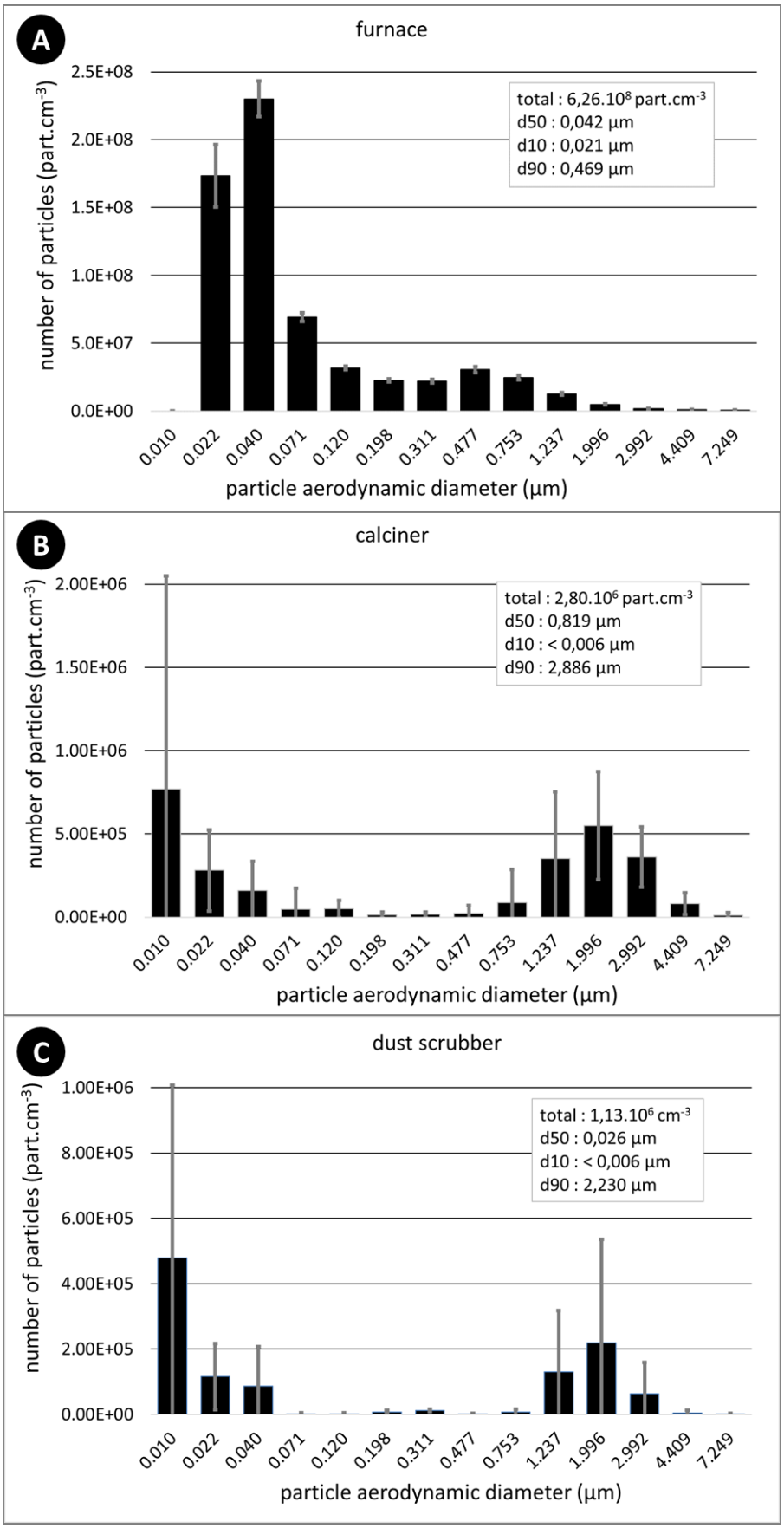

Figure 9. Particle size distribution of the aerosols sampled at different locations

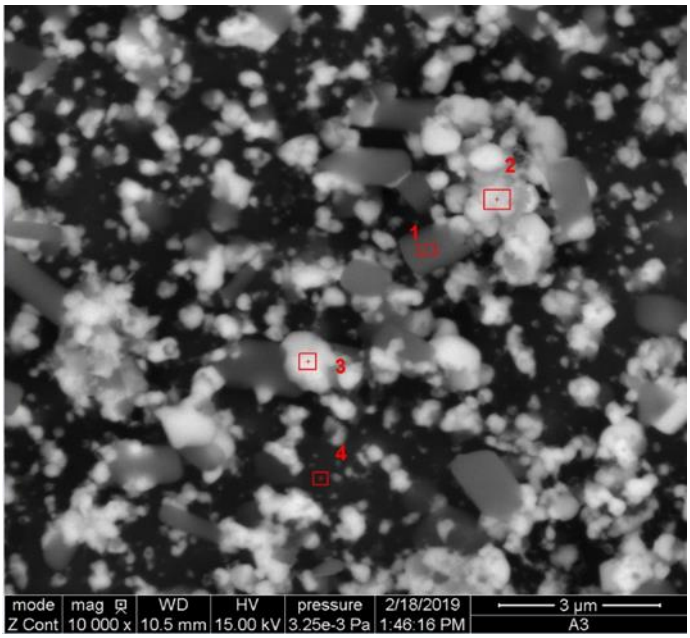

Figure 10. Morphology of submicronic particles from the furnace, observed with SEM

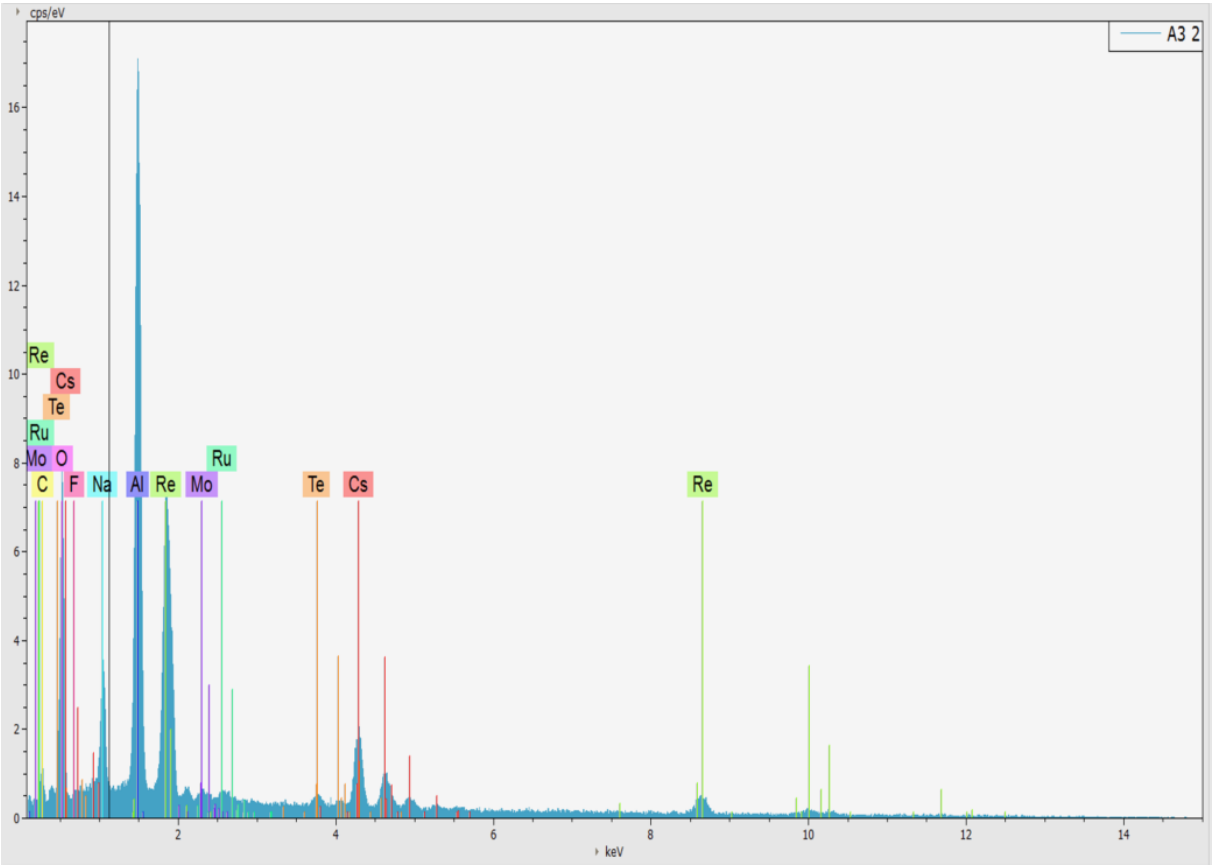

Figure 11. SEM-EDS spectra from Analysis n2 on Fig. 10

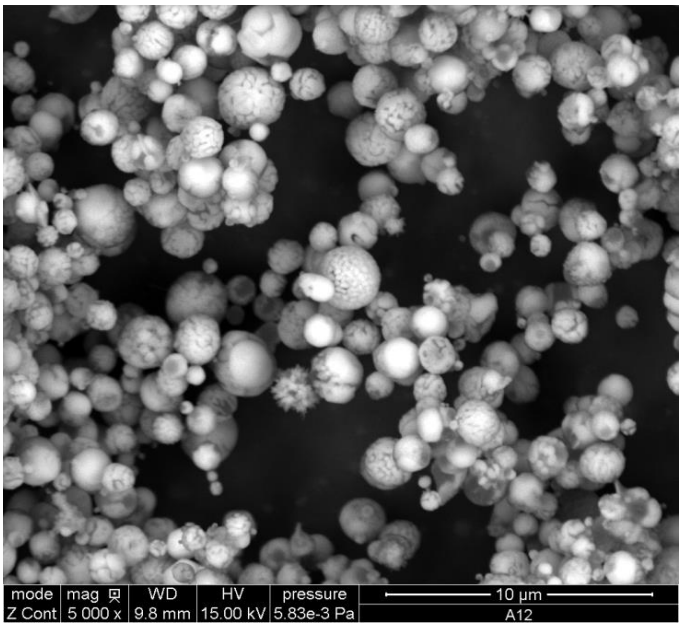

Figure 12. Morphology of micronic particles from the furnace, observed with SEM

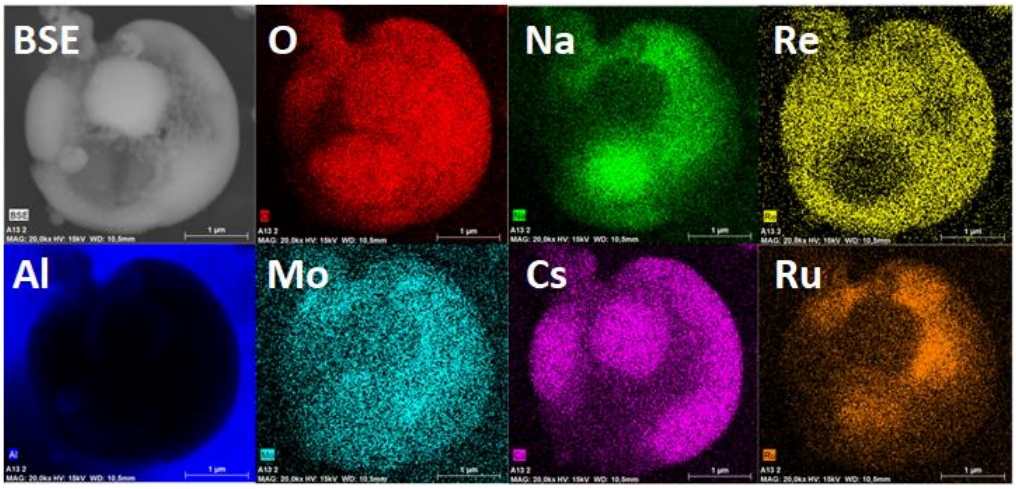

Figure 13. SEM-EDS mapping of a micronic particle from the furnace

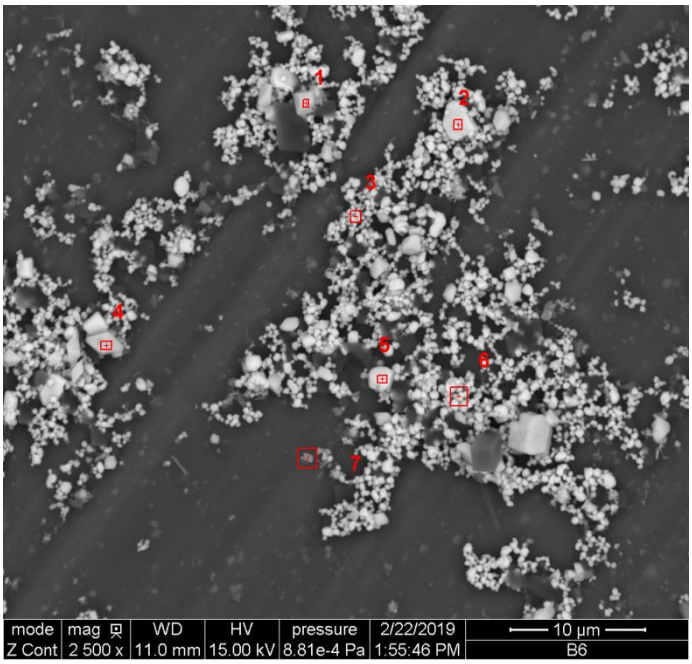

Figure 14. Morphology of micronic particles from the calciner, observed with SEM

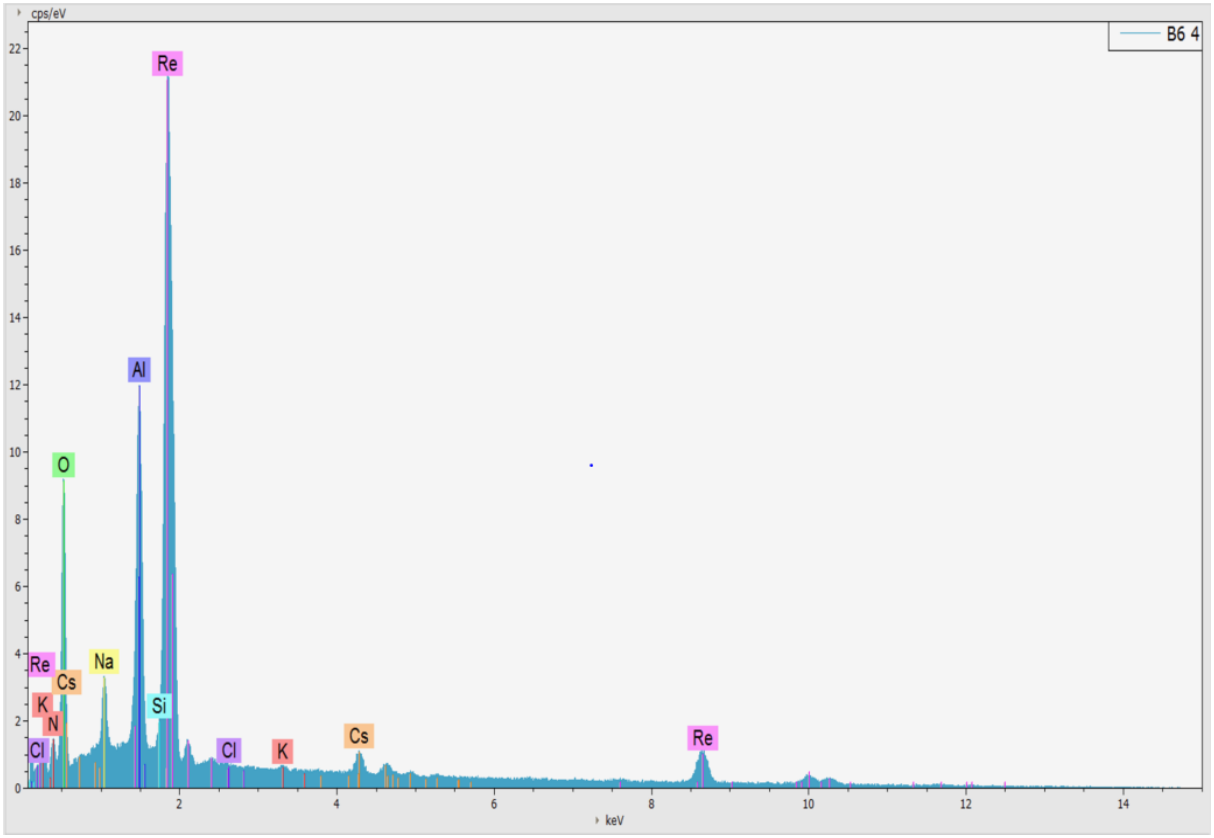

Figure 15. SEM-EDS spectra from Analysis n4 on Fig. 14

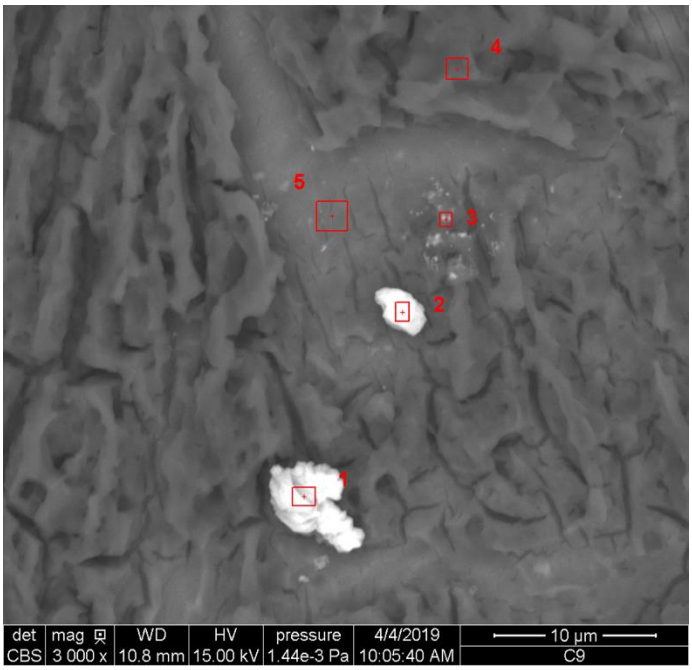

Figure 16. Morphology of micronic particles from the dust scrubber, observed with SEM

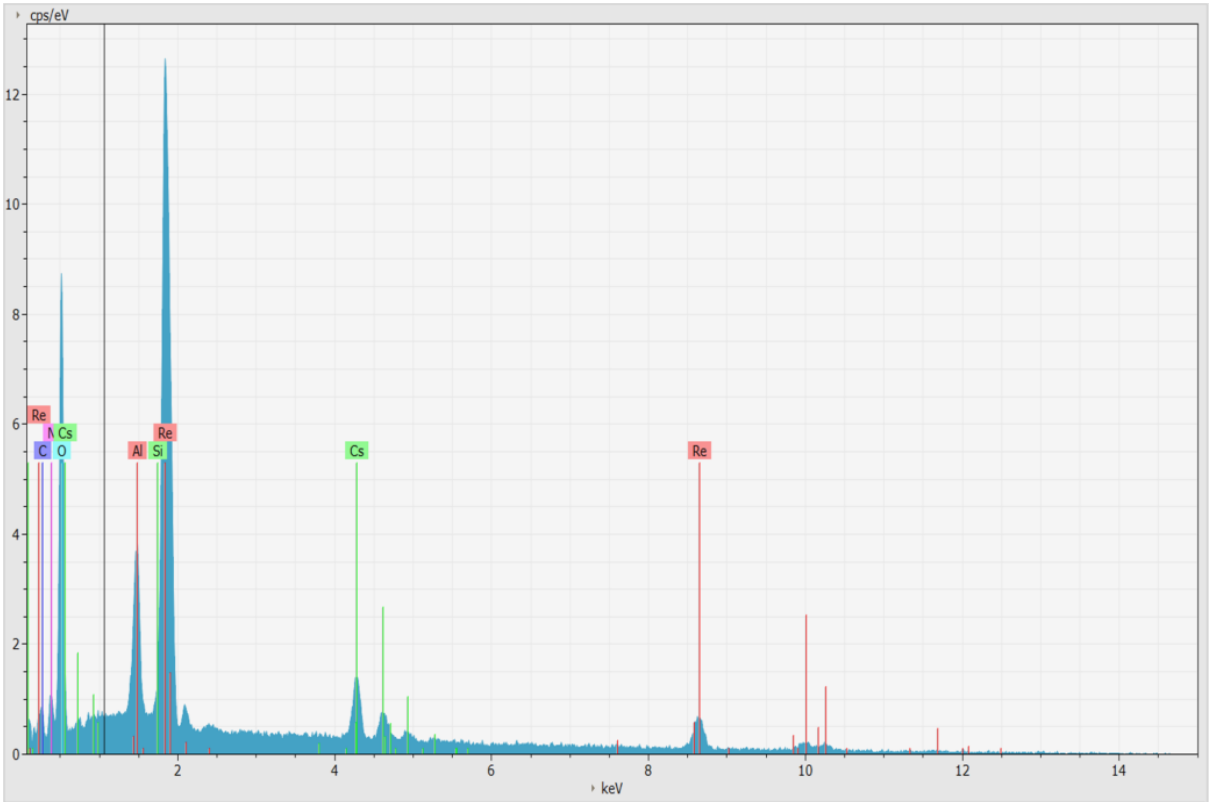

Figure 17. SEM-EDS spectra from Analysis n1 on Fig. 16

TABLES

Element	Product added to the waste solution	Oxides	Calcine composition (wt%)		Glass frit composition (wt%)	Final glass composition (wt%)	
			SSG	**HSG**		**SSG** F/V = 0.762	**HSG** F/V = 0.783
Al	$AlN_3O_9.9H_2O$	Al_2O_3	5.8	4.9	4.3	4.6	4.4
B	HBO_3	B_2O_3	0.2	0.2	18.2	13.9	14.2
Ba	BaN_2O_6	BaO	3.9	3.3	0	0.9	0.7
Ca	-	CaO	-	-	5.2	4.0	4.1
Cs	$CsNO_3$	Cs_2O	3.6	10.1	0	0.9	2.2
Fe	$FeN_3O_9.9H_2O$	Fe_2O_3	1.2	1.0	0	0.3	0.2
Li	-	Li_2O	-	-	2.6	2.0	2.0
Mo	MoO_3	MoO_3	9.0	7.6	0	2.1	1.6
Na	$NaNO_3$	Na_2O	21.3	17.9	7.0	10.4	9.4
Nd	$NdN_3O_9.6H_2O$	Nd_2O_3	34.1	28.7	0	8.0	6.3
Pd	PdN_2O_6	Pd	3.6	3.6	0	0.9	0.8
Re	$HReO_4$	ReO_2	1.3	8.4	0	0.3	1.8
Ru	$HN_4O_{10}Ru$	RuO_2	5.4	5.4	0	1.3	1.2
Si	-	SiO_2	-	-	58.8	44.8	46.1
Te	TeN_4O_{12}	TeO_2	0.6	0.5	0	0.2	0.1
Zn	-	ZnO	-	-	3.2	2.5	2.5
Zr	$ZrO_2.H_2O$	ZrO_2	10.0	8.4	0.7	2.9	2.4

Table 1. Formulation of the Slightly Spiked Glass (SSG) and the Highly Spiked Glass (HSG)

Element	Product added to the waste solution	Oxides	Calcine composition (wt%)	Glass frit composition (wt%)	Final glass composition (wt%) F/V = 0.741
Al	$AlN_3O_9.9H_2O$	Al_2O_3	5.9	4.3	4.7
B	HBO_3	B_2O_3	0.2	18.2	13.5
Ba	BaN_2O_6	BaO	3.9	0	1.0
Ca	-	CaO	-	5.2	3.9
Cs	$CsNO_3$	Cs_2O	5.0	0	1.3
Fe	$FeN_3O_9.9H_2O$	Fe_2O_3	10.8	0	2.8
Li	-	Li_2O	-	2.6	1.9
Mo	MoO_3	MoO_3	9.3	0	2.4
Na	$NaNO_3$	Na_2O	17.8	7.0	9.8
Nd	$NdN_3O_9.6H_2O$	Nd_2O_3	24.0	0	6.2
Pd	PdN_2O_6	Pd	3.1	0	0.8
Re	$HReO_4$	ReO_2	2.7	0	0.7
Ru	$HN_4O_{10}Ru$	RuO_2	5.0	0	1.3
Si	-	SiO_2	-	58.8	43.6
Te	TeN_4O_{12}	TeO_2	1.2	0	0.3
Zn	-	ZnO	-	3.2	2.4
Zr	$ZrO_2.H_2O$	ZrO_2	11.1	0.7	3.4

Table 2. Formulation of the Typical Simulant Glass (TSG)

Aerosol sampling point	**Gas temperature (°C)**	**Carrier gas flow ($L.h^{-1}$)**
furnace gas outlet	300	950
calciner gas outlet	130	18,560
dust scrubber gas outlet	95	19,350

Table 3. PSMU process data

APPENDIX A: PHOTOS OF THE SMALL-SCALE CALCINER (SSC)

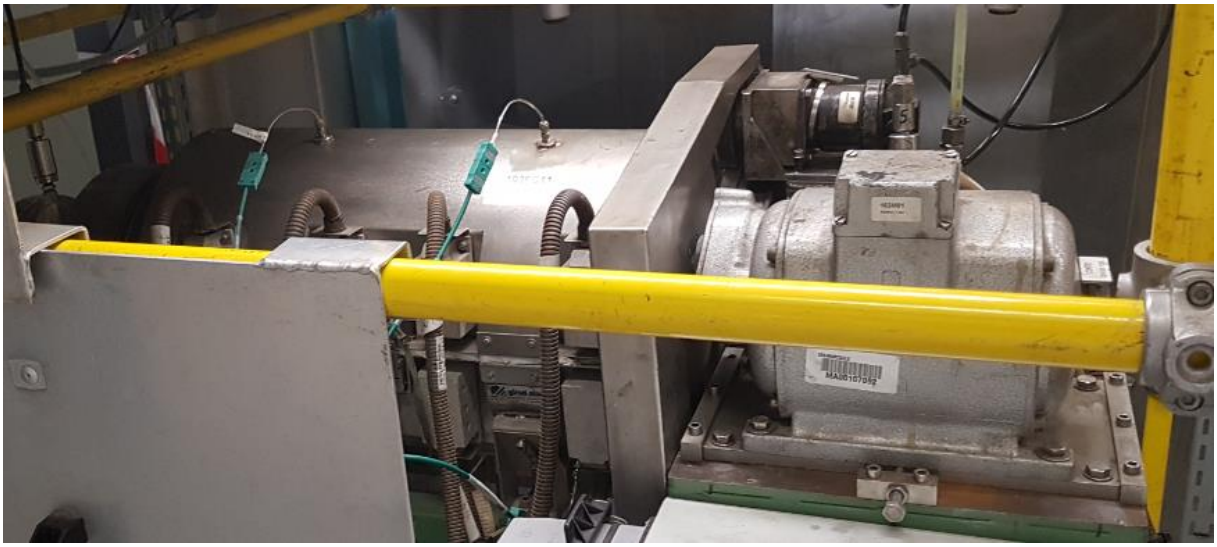

Figure A.1. Profile photo of the SSC

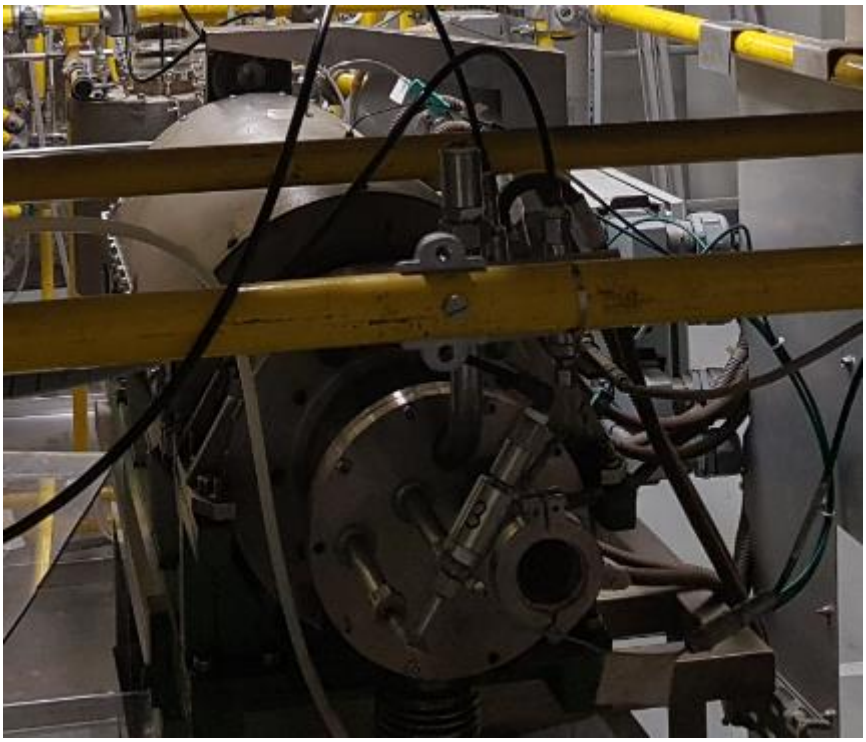

Figure A.2. Photo of the outlet of the SSC to the furnace

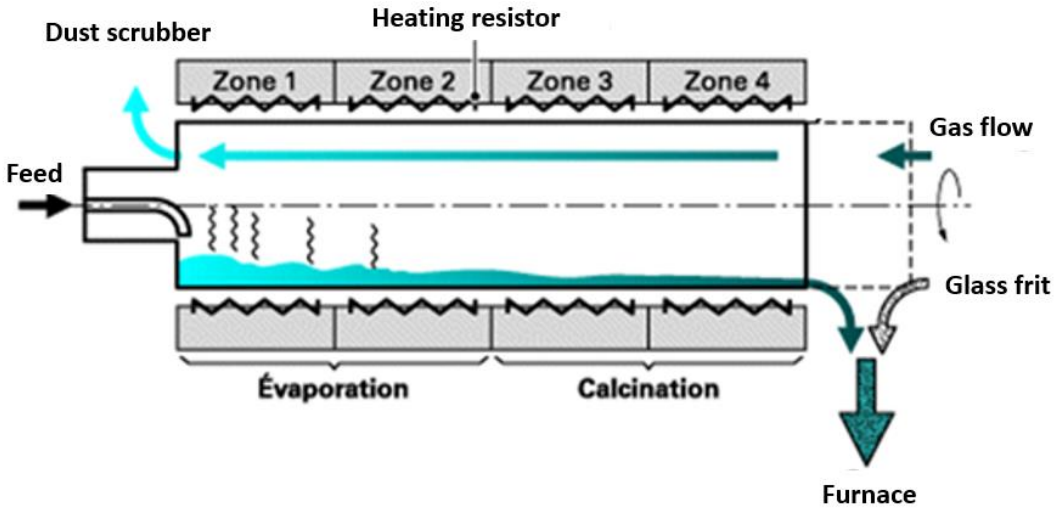

Figure A.3. Basic diagram of the calciner structure

APPENDIX B: PHOTO OF THE SOLIDIFICATION TREATMENT MOCK-UP (STREAM)

Figure B.1. Profile photo of the STREAM